BIOPHYSICS

A molecular sensor for cholesterol in the human serotonin$_{1A}$ receptor

G. Aditya Kumar[1†‡], Parijat Sarkar[1†], Tomasz Maciej Stepniewski[2,3†], Md. Jafurulla[1], Shishu Pal Singh[4], Jana Selent[2]*, Amitabha Chattopadhyay[1]*

Copyright © 2021 The Authors, some rights reserved; exclusive licensee American Association for the Advancement of Science. No claim to original U.S. Government Works. Distributed under a Creative Commons Attribution NonCommercial License 4.0 (CC BY-NC).

The function of several G protein–coupled receptors (GPCRs) exhibits cholesterol sensitivity. Cholesterol sensitivity of GPCRs could be attributed to specific sequence and structural features, such as the cholesterol recognition/interaction amino acid consensus (CRAC) motif, that facilitate their cholesterol-receptor interaction. In this work, we explored the molecular basis of cholesterol sensitivity exhibited by the serotonin$_{1A}$ receptor, the most studied GPCR in the context of cholesterol sensitivity, by generating mutants of key residues in CRAC motifs in transmembrane helix 2 (TM2) and TM5 of the receptor. Our results show that a lysine residue (K101) in one of the CRAC motifs is crucial for sensing altered membrane cholesterol levels. Insights from all-atom molecular dynamics simulations showed that cholesterol-sensitive functional states of the serotonin$_{1A}$ receptor are associated with reduced conformational dynamics of extracellular loops of the receptor. These results constitute one of the first reports on the molecular mechanism underlying cholesterol sensitivity of GPCRs.

INTRODUCTION

G protein–coupled receptors (GPCRs) represent the largest group of integral membrane proteins in the human proteome and convey diverse extracellular signals to the cellular interior (*1*). They act as popular drug targets in all clinical areas and account for ~40% of current drug targets (*2*). The sensitivity of GPCRs toward their immediate membrane lipid microenvironment constitutes an exciting yet poorly resolved area of contemporary GPCR biology. Cholesterol is a vital membrane lipid in higher eukaryotes that plays a crucial role in a large number of cellular functions (*3*). The fine-tuned structural attributes of cholesterol allow its interaction with membrane proteins with high specificity (*4*, *5*). The role of membrane cholesterol in the function of several GPCRs has been reported (*6*–*10*). We have previously shown that the serotonin$_{1A}$ receptor, a representative class A neurotransmitter GPCR (*11*, *12*), exhibits sensitivity toward membrane cholesterol in terms of its organization, dynamics, function, and trafficking (*13*–*22*). However, the mechanistic basis underlying the cholesterol-sensitive GPCR function remains elusive. In other words, what are the molecular determinants that enable GPCRs to perceive and respond to changes in membrane cholesterol levels in terms of altered functional consequences? High-resolution structures of cholesterol-bound GPCRs offer crucial insight into the interaction of cholesterol with these receptors (*5*, *10*, *23*, *24*) and the promise of novel drug discovery (*25*). In this context, cholesterol interaction motifs represent putative sites on receptors that could be involved in facilitating specific interaction (*26*–*28*). Among these, the cholesterol recognition/interaction amino acid consensus (CRAC) motif is one of the most well studied and is characterized by a linear sequence of amino acids -L/V-(X)$^{1-5}$-Y-(X)$^{1-5}$-R/K- (from the N terminus to the C terminus of the protein), where (X)$^{1-5}$ represents between one and five residues of any amino acid (*28*–*31*).

In the case of GPCRs, we previously reported the presence of CRAC motifs in three representative class A GPCRs (rhodopsin, β_2-adrenergic receptor, and serotonin$_{1A}$ receptor), all of which display cholesterol-sensitive function (*30*). Specifically, CRAC motifs in serotonin$_{1A}$ receptors were shown to be conserved across vertebrates, which further highlights the evolutionary significance of these motifs in serotonin$_{1A}$ receptor function (*30*). With an overall objective to explore the mechanistic basis underlying the cholesterol-sensitive function of the serotonin$_{1A}$ receptor, in this work, we explored the role of CRAC motifs in transmembrane helix 2 (TM2) and TM5 of the serotonin$_{1A}$ receptor. Using complementary approaches [site-directed mutagenesis, measurement of cellular signaling, and all-atom molecular dynamics (MD) simulations], we show that a key lysine residue (K101) forming part of the CRAC motif in TM2 of the serotonin$_{1A}$ receptor is crucial in sensing altered membrane cholesterol levels. We further show that cholesterol-sensitive functional states of the serotonin$_{1A}$ receptor are associated with reduced conformational dynamics of the extracellular loops (ECLs) of the receptor. To the best of our knowledge, these results represent the first comprehensive report on the underlying molecular mechanism associated with cholesterol sensitivity of GPCRs.

RESULTS

Cholesterol-dependent signaling by serotonin$_{1A}$ receptors

We have stably expressed the human serotonin$_{1A}$ receptor in human embryonic kidney (HEK) 293 cells and demonstrated that the receptor exhibits characteristic ligand binding, G-protein coupling, lateral dynamics, and intracellular trafficking, highlighting functional receptor expression in these cells (*32*, *33*). As a downstream response to agonist stimulation, the serotonin$_{1A}$ receptor is known to activate the G_i/G_o class of G-proteins in HEK-293 cells (*34*). This results in the inhibition of adenylyl cyclase activity that leads to a reduction in cellular cyclic adenosine 3′,5′-monophosphate (cAMP) levels (*35*) (see Fig. 1A). We monitored the effect of serotonin (agonist) stimulation

[1]CSIR-Centre for Cellular and Molecular Biology, Uppal Road, Hyderabad 500 007, India. [2]Research Programme on Biomedical Informatics (GRIB), Department of Experimental and Health Sciences of Pompeu Fabra University (UPF)-Hospital del Mar Medical Research Institute (IMIM), 08003 Barcelona, Spain. [3]Faculty of Chemistry, Biological and Chemical Research Centre, University of Warsaw, Warsaw, Poland. [4]National Centre for Biological Sciences, UAS-GKVK Campus, Bellary Road, Bengaluru 560 065, India.
*Corresponding author. Email: amit@ccmb.res.in (A.C.); jana.selent@upf.edu (J.S.)
†These authors contributed equally to this work.
‡Present address: Department of Pharmacology, University of Michigan Medical School, Ann Arbor, MI 48109, USA.

Downloaded from http://advances.sciencemag.org/ on July 23, 2021

on reduction in cAMP levels in HEK-293 cells stably expressing the wild-type human serotonin$_{1A}$ receptor using a fluorescence resonance energy transfer (FRET)–based assay (*36*, *37*) (see Materials and Methods for more details). This assay is based on estimating agonist-induced reduction in forskolin-stimulated cAMP levels. Since basal cellular cAMP levels are low and a further reduction in their levels is difficult to measure, we enhanced cellular cAMP levels using forskolin, which activates adenylyl cyclase independent of G-proteins. As shown in Fig. 1B, forskolin stimulation resulted in ~70% increase in cellular cAMP levels. Treatment with 10 μM serotonin led to a reduction in the forskolin-stimulated enhancement of cAMP levels (see Fig. 1B).

Depletion of membrane cholesterol offers a convenient strategy to monitor cholesterol dependence of GPCR function (*13*, *14*, *38*). We used methyl-β-cyclodextrin (MβCD), a water-soluble carbohydrate polymer that selectively and efficiently extracts cholesterol from membranes (*39*, *40*), to deplete membrane cholesterol from HEK-293 cells. To explore the cholesterol sensitivity of serotonin$_{1A}$ receptor signaling, we measured serotonin-induced reduction in cAMP levels in cholesterol-depleted cells. Figure 2A shows membrane cholesterol content in HEK-293 cells expressing the serotonin$_{1A}$ receptor upon treatment with 10 mM MβCD. We observed ~40% reduction in membrane cholesterol content in cells upon treatment with MβCD. The reduction in cellular cAMP content upon serotonin treatment relative to forskolin-stimulated levels is shown in Fig. 2B. The figure shows that control (untreated) cells exhibited ~71% reduction in cAMP levels upon treatment with serotonin. As shown in Fig. 2B and fig. S1, the serotonin-induced reduction in cAMP levels was inhibited upon depletion of membrane cholesterol. This implies that membrane cholesterol depletion inhibits serotonin-mediated signaling by the serotonin$_{1A}$ receptor and highlights the cholesterol sensitivity of serotonin$_{1A}$ receptor function.

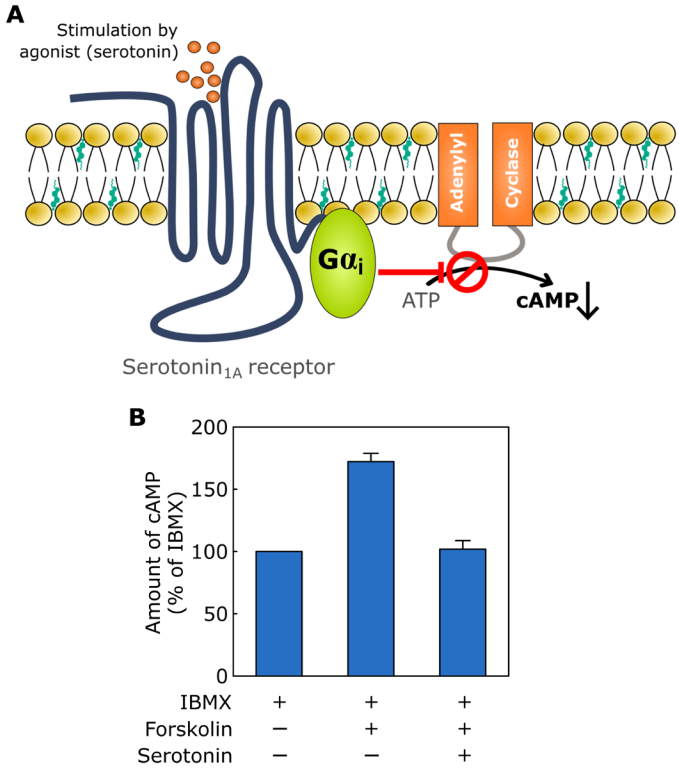

Fig. 1. Reduction in intracellular cAMP levels upon agonist stimulation of serotonin$_{1A}$ receptors. (**A**) A schematic representation showing cAMP signaling by the serotonin$_{1A}$ receptor. Upon agonist (serotonin) stimulation, the serotonin$_{1A}$ receptor negatively regulates adenylyl cyclase activity via the inhibitory G-protein Gα_i, resulting in a reduction in cellular cAMP levels. ATP, adenosine 5′-triphosphate. (**B**) Estimation of cellular cAMP levels in HEK-293 cells stably expressing wild-type human serotonin$_{1A}$ receptors using a FRET-based assay. Cells were incubated with 10 μM forskolin to enhance the basal levels of intracellular cAMP. The ability of the serotonin$_{1A}$ receptor to inhibit forskolin-stimulated increase in cAMP levels upon treatment with 10 μM serotonin was assessed. Data are normalized to cAMP levels in the presence of 50 μM IBMX (phosphodiesterase inhibitor). Data represent means ± SE of at least six independent experiments. See Materials and Methods for further details.

CRAC motif mutants of the serotonin$_{1A}$ receptor

To explore the molecular determinants of cholesterol-sensitive serotonin$_{1A}$ receptor signaling, we monitored the role of CRAC motifs in conferring such sensitivity. For this, we selectively mutated key charged and aromatic amino acid residues in these motifs. The rationale behind our approach was that if an amino acid residue is involved in sensing membrane cholesterol, a receptor harboring a mutation in that residue should exhibit functional readouts that would remain invariant with changes in membrane cholesterol content. In other words, mutations in amino acids that are involved in sensing membrane cholesterol should not support cholesterol-dependent changes in receptor signaling as observed in the case of the wild-type receptor. Cholesterol interaction motifs in membrane receptors facilitate the interaction of receptors with cholesterol via aromatic amino acid residues that have been suggested to interact with ring D of the fused steroid ring of cholesterol (*26*, *27*). On the other hand, positively charged residues in the CRAC motif have been proposed to be involved in electrostatic interactions with the 3β-hydroxyl group of cholesterol (*27*, *41*, *42*). To understand the molecular basis of the cholesterol sensitivity exhibited by the serotonin$_{1A}$ receptor, we generated mutants of key amino acid residues in CRAC

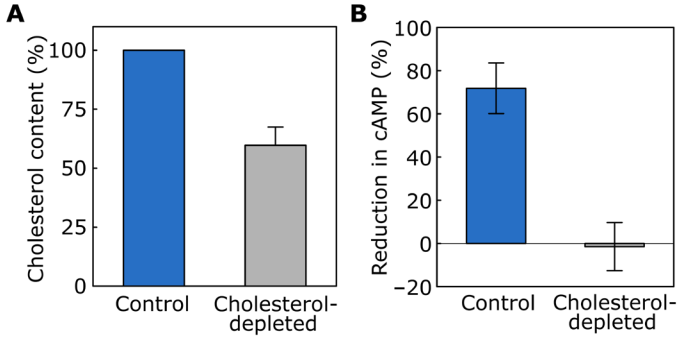

Fig. 2. Effect of cholesterol depletion on cAMP signaling by the serotonin$_{1A}$ receptor. (**A**) Cholesterol was depleted from HEK-293 cells stably expressing wild-type serotonin$_{1A}$ receptors by incubating cells with 10 mM MβCD for 30 min in serum-free medium. Membrane cholesterol content upon treatment with MβCD is shown. Values are normalized to the cholesterol content of control (untreated) cells. Data represent means ± SE of three independent experiments. (**B**) Reduction in cAMP upon incubation of cells with 10 μM serotonin was monitored in control (untreated, blue) and cholesterol-depleted (MβCD-treated, gray) cells. Values are expressed as percentage reduction in cAMP levels due to agonist stimulation of wild-type serotonin$_{1A}$ receptors. Data represent means ± SE of at least three independent experiments. See Materials and Methods for further details.

Downloaded from http://advances.sciencemag.org/ on July 23, 2021

motif I (in TM2) and CRAC motif II (in TM5) of the receptor (see Fig. 3A). For this, we generated four single mutants, Y96S and K101A (in CRAC motif I), Y215S and R220A (in CRAC motif II), and two double mutants, Y96S + Y215S and K101A + R220A, and subsequently stably expressed them in HEK-293 cells (Fig. 3A; see Materials and Methods for details). Confocal microscopic imaging at a midplane section of HEK-293 cells expressing wild-type and mutant serotonin$_{1A}$ receptors showed that receptors were expressed on the plasma membrane (see fig. S2). We further quantified the expression of the wild type and mutants of the serotonin$_{1A}$ receptor on the plasma membrane of HEK-293 cells using a flow cytometric assay. As shown in fig. S3, all CRAC motif mutants of the serotonin$_{1A}$ receptor are expressed on the plasma membrane, although to varying extents.

CRAC motifs in signaling by the serotonin$_{1A}$ receptor

To explore whether mutations in CRAC motifs of the serotonin$_{1A}$ receptor affect their downstream signaling ability, we monitored reduction in cAMP levels in these mutants upon treatment with serotonin. As shown in Fig. 4 (blue bars) and fig. S4A, under normal conditions, a considerable reduction in serotonin-induced cAMP levels was observed in CRAC motif mutants similar to wild-type receptors, suggesting that these mutants retain their downstream signaling ability. The mechanistic basis of cholesterol sensitivity of the serotonin$_{1A}$ receptor downstream signaling was explored by monitoring the effect of cholesterol depletion on signaling by CRAC motif mutants. Figure 3B shows the membrane cholesterol content in HEK-293 cells expressing CRAC motif mutants of the serotonin$_{1A}$ receptor upon treatment with 10 mM MβCD. As discussed above, we observed ~40% reduction in membrane cholesterol content in wild-type cells upon treatment with MβCD. The extent of cholesterol depletion in HEK-293 cells expressing CRAC motif mutants was similar to cells expressing wild-type receptors and consistent across all mutants (see Fig. 3B). Depletion of membrane cholesterol did not exhibit a notable effect on the plasma membrane localization of the wild-type and mutant serotonin$_{1A}$ receptors (see fig. S2).

We observed inhibition in cAMP signaling upon cholesterol depletion in the case of Y96S, Y215S, and R220A mutants (see Fig. 4, gray bars, and fig. S4B). These three mutants exhibited a downstream signaling response to cholesterol depletion similar to wild-type receptors, suggesting that Y96, Y215, and R220 residues are not involved in conferring cholesterol sensitivity to the serotonin$_{1A}$ receptor. As expected, the Y96S + Y215S double mutant exhibited a trend in downstream signaling similar to the wild-type receptor and the constituent single mutants (Fig. 4 and figs. S4B and S5). Strikingly, the K101A mutant did not exhibit any appreciable change in downstream signaling response upon cholesterol depletion, implying that its signaling efficiency was independent of cholesterol content. Notably, the K101A + R220A double mutant displayed cholesterol insensitivity as observed in the case of the K101A single mutant (see Fig. 4 and figs. S4B and S5). Together, our results show that the cholesterol sensitivity observed in serotonin$_{1A}$ receptor signaling is conferred by the K101 residue in CRAC motif I of the receptor.

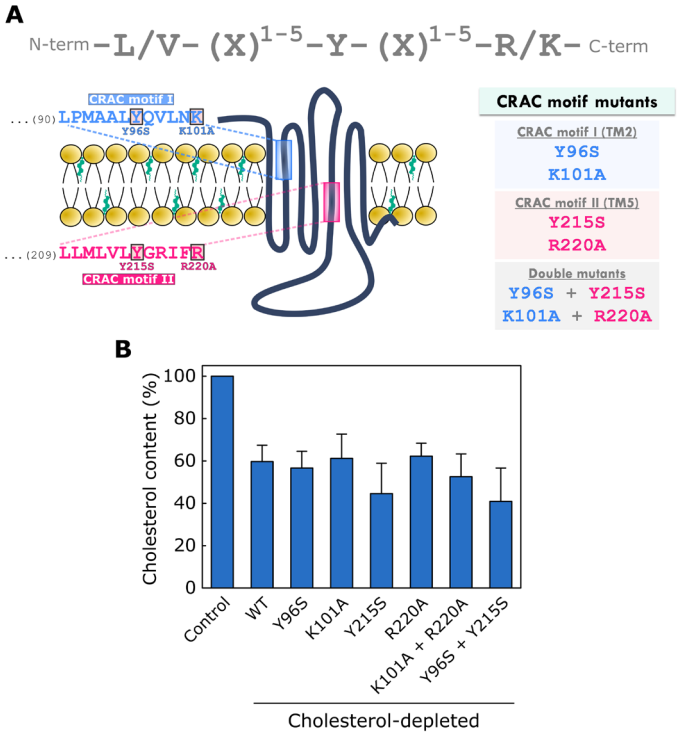

Fig. 3. CRAC motif mutants of the serotonin$_{1A}$ receptor. (**A**) The linear sequence of amino acids constituting the CRAC motif is shown on top. The serotonin$_{1A}$ receptors with CRAC motifs in TM2 (CRAC motif I) and TM5 (CRAC motif II) are highlighted in blue and pink, respectively. The amino acid sequences corresponding to CRAC motifs I and II of the serotonin$_{1A}$ receptor are indicated. To study the role of these motifs in rendering cholesterol sensitivity to the serotonin$_{1A}$ receptor, we generated four single (Y96S, K101A, Y215S, and R220A) and two double mutants (Y96S + Y215S and K101A + R220A) in CRAC motifs of the receptor (highlighted with a box and listed on the right). (**B**) Membrane cholesterol content of HEK-293 cells expressing wild-type (WT) and CRAC motif mutant serotonin$_{1A}$ receptors upon treatment with 10 mM MβCD. Values are normalized to the cholesterol content of the respective untreated cells (control). Data represent means ± SE of three independent experiments. See Materials and Methods for further details.

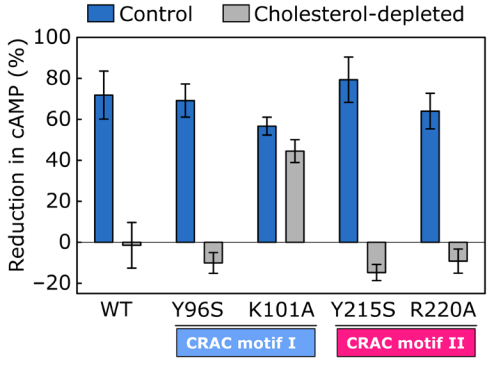

Fig. 4. Role of crucial amino acid residues of the CRAC motif in cholesterol sensitivity of serotonin$_{1A}$ receptor signaling. The ability of the wild-type and mutant serotonin$_{1A}$ receptors to inhibit forskolin-stimulated increase in cAMP levels upon treatment with 10 μM serotonin was monitored. Reduction in cAMP in control (untreated, blue) and cholesterol-depleted (MβCD-treated, gray) cells is expressed as a percentage of cAMP levels in cells incubated with 10 μM forskolin. Cholesterol sensitivity to signaling is retained in the Y96S, Y215S, and R220A mutants [similar to wild-type (WT) receptor]. However, this sensitivity is lost in the case of the K101A mutant, suggesting a possible role of K101 (in CRAC motif I) in conferring cholesterol sensitivity to serotonin$_{1A}$ receptor function. Data represent means ± SE of at least three independent experiments. See Materials and Methods for further details.

Downloaded from http://advances.sciencemag.org/ on July 23, 2021

Binding of cholesterol to the K101 residue in CRAC motif I

To obtain structural insights into the observed cholesterol-sensitive signaling by the serotonin$_{1A}$ receptor, we carried out 4 × 2 μs all-atom NVT MD simulations of the receptor in complex with its native agonist serotonin in 1-palmitoyl-2-oleoyl-*sn*-glycero-3-phosphocholine (POPC) membranes with 33% cholesterol (termed POPC/chol). We computed the occupancy map for cholesterol on the serotonin$_{1A}$ receptor and analyzed the preferred binding sites for cholesterol on the receptor. We observed that cholesterol favored a site near K101 during at least 20% of the simulations (see yellow volume in Fig. 5A). Detailed analysis of the binding modality showed that the bound cholesterol molecule is sandwiched between TM1 and TM2 in a binding groove formed by multiple hydrophobic residues (Fig. 5B). In this binding mode, cholesterol can establish polar interactions

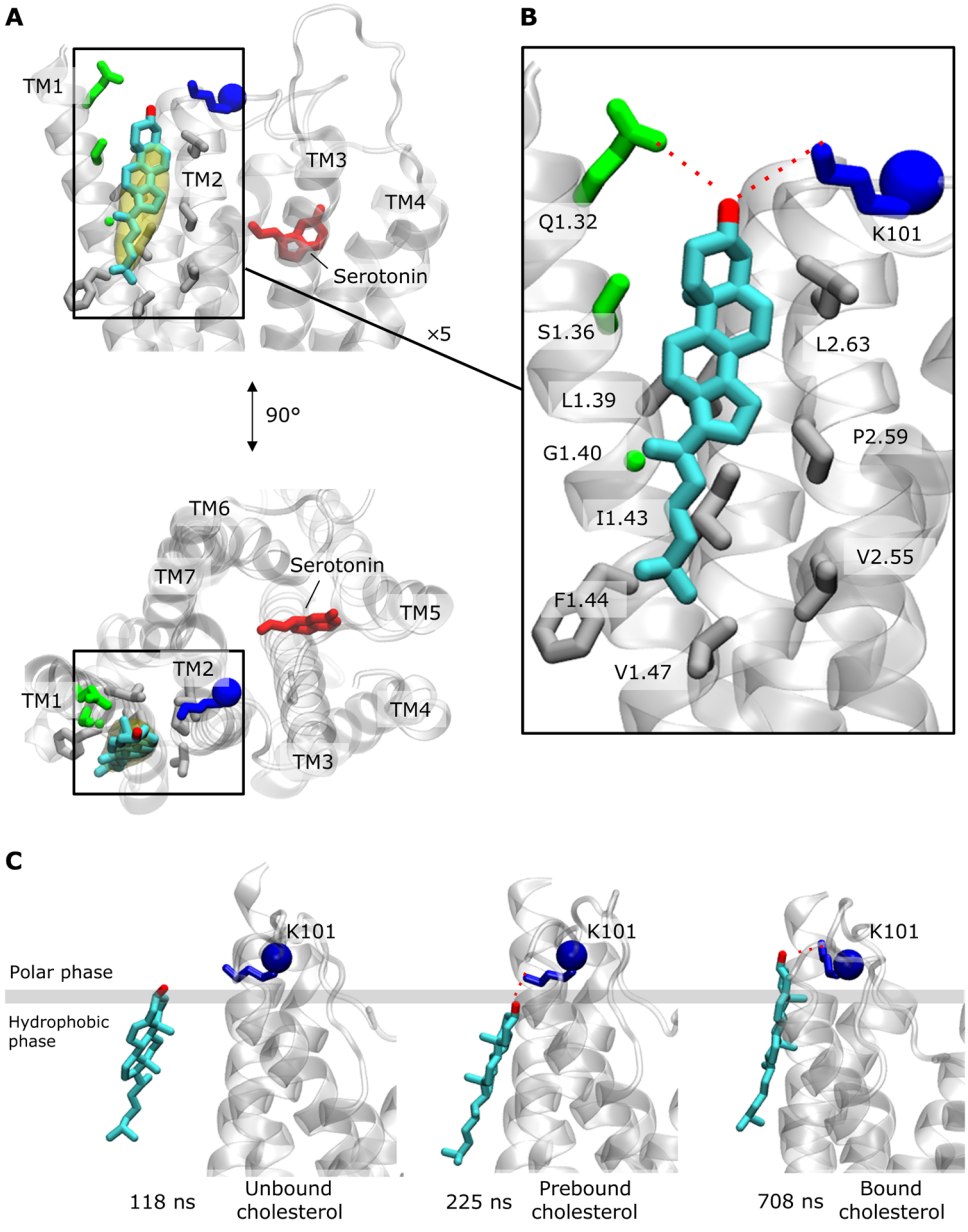

Fig. 5. Binding dynamics of cholesterol to the serotonin$_{1A}$ receptor. (**A**) Binding mode of cholesterol to the serotonin$_{1A}$ receptor detected in MD simulations. Cholesterol occupancy (at a 0.2 threshold) in the vicinity of K101 residue (shown in dark blue) in CRAC motif I is plotted as a yellow surface. A cholesterol molecule bound in this predicted area is represented in cyan. Serotonin is depicted in red. (**B**) Residues in contact with cholesterol in the identified binding mode. Residues (except K101) are numbered according to the Ballesteros-Weinstein scheme. Polar interactions with cholesterol are depicted as red dotted lines. Nonpolar, polar, and positively charged residues on the serotonin$_{1A}$ receptor are colored in gray, green, and dark blue, respectively. The Cα of the K101 residue in serotonin$_{1A}$ receptor is depicted in van der Waals representation (dark blue). (**C**) The K101 residue facilitates cholesterol binding to the serotonin$_{1A}$ receptor. Snapshots along the binding pathway of cholesterol to the serotonin$_{1A}$ receptor are shown. When cholesterol is within sufficient proximity to the binding site (unbound cholesterol, 118 ns), it forms initial contacts with K101 (prebound cholesterol, 225 ns). In such a state, cholesterol is initially tethered to the serotonin$_{1A}$ receptor, and later, it can transit into a tighter binding mode (bound cholesterol, 708 ns) in which, besides K101, it interacts with other residues in the serotonin$_{1A}$ receptor. See Materials and Methods for further details.

Downloaded from http://advances.sciencemag.org/ on July 23, 2021

with Q1.32 and K101 residues (see Fig. 5B). In addition, our results showed that K101 forms the first recognition point that drives cholesterol interaction (see Fig. 5C, prebound cholesterol) with the receptor. In this state, the cholesterol molecule remains bound mainly to the K101 residue for extended periods of time. In the prebound modality, the methyl groups on the β face have no strict orientation. However, upon transition to the fully bound state, they turn around to tightly fit into the binding groove where they interact with hydrophobic residues on the serotonin$_{1A}$ receptor (see Fig. 5C, bound cholesterol). The first recognition event with K101 is preceded by the transition of one cholesterol from the bulk toward the serotonin$_{1A}$ receptor in the upper bilayer leaflet (Fig. 5C, unbound to prebound cholesterol). During this transition, the polar headgroup of cholesterol firmly interacts with the phosphocholine part of the lipid bilayer (fig. S6). Together, these observations complement our experimental results on the role of the K101 residue in rendering cholesterol sensitivity to the serotonin$_{1A}$ receptor (see Fig. 4).

ECL dynamics in cholesterol-sensitive receptor function

With the aim of exploring the molecular interplay between cholesterol interaction at the K101 residue and agonist-induced signaling by the serotonin$_{1A}$ receptor, we generated additional 4 × 2 μs NVT simulations starting from the observed cholesterol-bound receptor state and filtered our simulations based on the presence of cholesterol in the proximity of the K101 residue. We compared these frames with another set of 4 × 2 μs of NVT simulations of the serotonin$_{1A}$ receptor in POPC membranes without cholesterol (termed POPC). As shown in Fig. 6A, analysis of receptor conformational dynamics quantified as root mean square fluctuation (RMSF) revealed higher stability of ECL1 in POPC/chol membranes (cholesterol-bound state of the receptor) relative to POPC membranes (cholesterol-unbound state of the receptor). Differences in the observed conformational dynamics can be appreciated by plotting structural snapshots along the simulations into one structural depiction (see Fig. 6A, compare left and right). Our data indicate that cholesterol binding limits ECL1 mobility by forming polar interactions with the K101 residue (as highlighted by red dotted lines in Fig. 5B), which tether the loop in a specific conformation. This observation raised the interesting possibility that the cholesterol sensitivity in serotonin$_{1A}$ receptor function could be due to the stabilization of ECL1 conformational dynamics by cholesterol. To test this hypothesis, we simulated the K101A mutant of the serotonin$_{1A}$ receptor in POPC and POPC/chol membranes. As shown in Fig. 4, a mutation in the K101 residue (K101A) renders the serotonin$_{1A}$ receptor insensitive to changes in membrane cholesterol. We observed that ECL1 of the K101A mutant assumes a helical conformation in both POPC and POPC/chol membranes, although less extensively in the case of POPC (see Fig. 6B). Notably, such a conformation was not explored by ECL1 of the wild-type serotonin$_{1A}$ receptor. To further understand the impact of a helical conformation on ECL1 stability of the K101A mutant, we filtered out simulation frames where the loop adopted a helical conformation (Fig 6B, right). Analysis of ECL1 conformational dynamics of the K101A mutant (in both POPC and POPC/chol membranes) yielded RMSF values comparable to values observed for wild-type receptors in POPC/chol membranes. Together, these observations suggest that K101A-induced helical conformation promotes ECL1 stability in a manner analogous to the stabilization of ECL1 of the wild-type serotonin$_{1A}$ receptor in the presence of cholesterol. In other words, cholesterol-induced reduction in ECL1 conformational dynamics for the wild-type serotonin$_{1A}$ receptor (Fig. 6A, left) could serve as a molecular determinant of serotonin$_{1A}$ receptor signaling. As a corollary, upon mutating the cholesterol-sensing K101 residue to alanine, the induction of a helical conformation leads to reduced ECL1 conformational dynamics in cholesterol-containing membranes (POPC/chol) and in membranes without cholesterol (POPC) (Fig. 6B, right), thereby stabilizing a signaling state of the receptor independent of membrane cholesterol (see Figs. 4 and 6B, right).

In the next step, we assessed whether ECL1 conformational dynamics could be correlated to global structural changes within the receptor that could be associated with differential signaling states of the receptor. As shown in Fig. 6C, our simulations show that in the case of the wild-type serotonin$_{1A}$ receptor in POPC membranes (which corresponds to a nonsignaling state of the receptor), fluctuations in ECL1 propagate to other ECL regions as indicated by higher RMSF values for ECL2 and ECL3 (maroon bars), compared to the wild-type receptor in POPC/chol membranes (orange bars) and the K101A mutant in either POPC (olive bars) or POPC/chol (green bars) membranes (all of which correspond to the signaling state of the receptor).

DISCUSSION

The sensitivity of GPCRs to membrane cholesterol constitutes an exciting area of research in GPCR biology (*7*–*10*). The function of several GPCRs has been shown to be intimately dependent on membrane cholesterol. For example, we have previously shown that the serotonin$_{1A}$ receptor exhibits sensitivity toward membrane cholesterol in terms of its organization, dynamics, and function (*13*–*20*, *22*). Such cholesterol dependence of GPCRs could be attributed to structural features of these receptors that could facilitate their preferential association with membrane cholesterol. In this backdrop, cholesterol interaction motifs such as the CRAC motif offer putative interaction sites on GPCRs that could facilitate the cholesterol-sensitive function of these receptors (*27*, *28*). We previously reported the presence of conserved CRAC motifs in TM2, TM5, and TM7 of the serotonin$_{1A}$ receptor (*30*). To understand the molecular basis of the cholesterol sensitivity exhibited by the serotonin$_{1A}$ receptor, in this work, we generated mutants of crucial amino acid residues in CRAC motif I (in TM2) and CRAC motif II (in TM5) of the receptor (see Fig. 3A). We chose not to mutate any residue in CRAC motif III (in TM7) since this motif overlaps with the NPXXY motif, which acts as a conserved microswitch involved in receptor activation (*1*, *43*, *44*). It has been suggested that the central tyrosine residue of the CRAC motif could interact with the fused steroid ring of cholesterol (*4*, *26*). The interfacial localization of aromatic residues such as tyrosine is a unique feature of transmembrane proteins (*45*). We chose to mutate tyrosine residues of CRAC motifs I and II (in TM2 and TM5, respectively) to serine, since such a mutation would preserve the hydrogen bonding ability within a helix such that the overall transmembrane helical structure is maintained (*46*). Our results show that the functional sensitivity of the serotonin$_{1A}$ receptor to membrane cholesterol is lost when the residue K101 in CRAC motif I is mutated (in both single and double mutants), indicating the role of K101 as a molecular sensor of membrane cholesterol.

Downloaded from http://advances.sciencemag.org/ on July 23, 2021

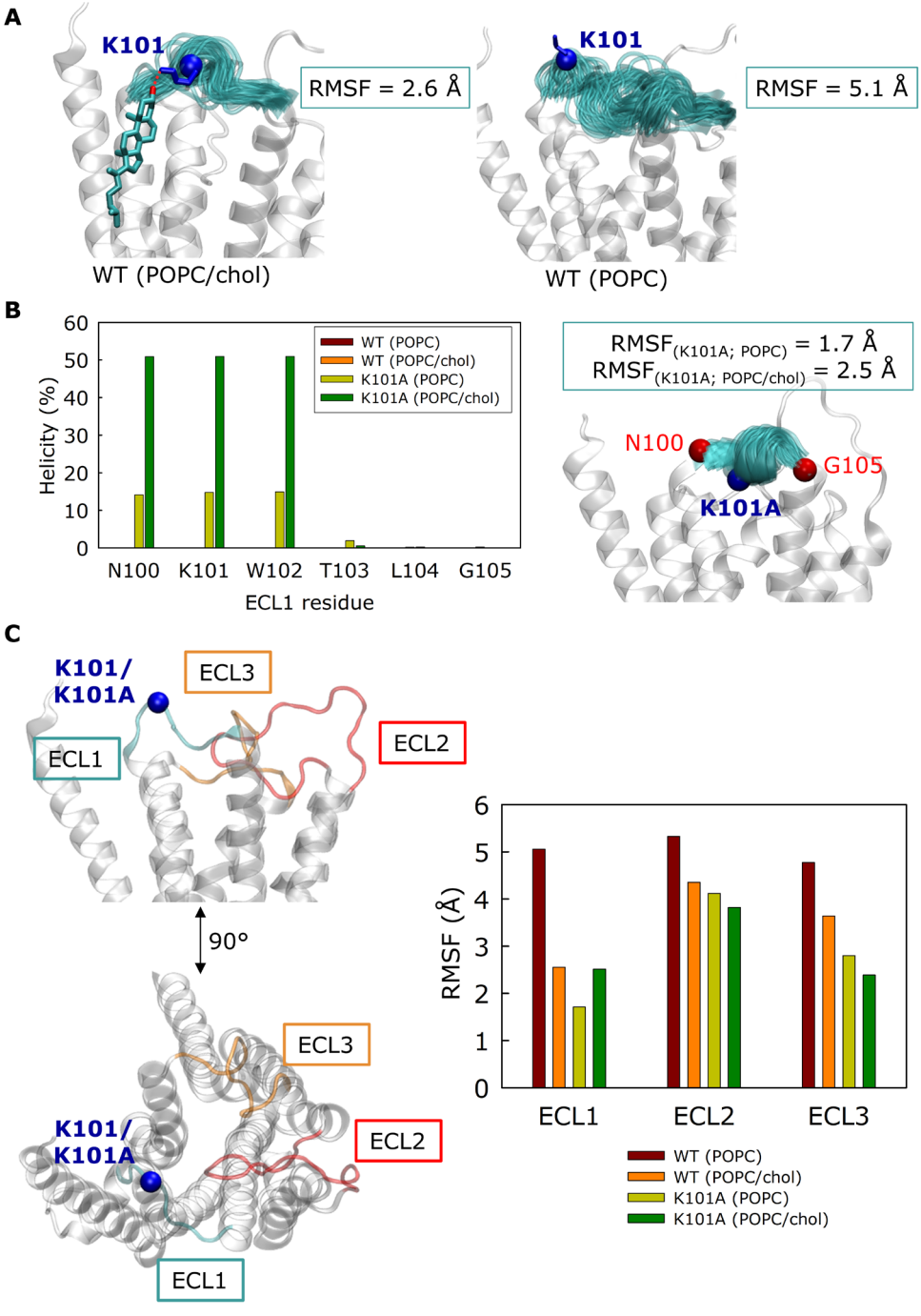

Fig. 6. Cholesterol sensitivity of the serotonin$_{1A}$ receptor correlates with conformational dynamics of ECLs. (**A**) Conformational states of ECL1 in frames of the serotonin$_{1A}$ receptor with cholesterol bound (left) and the serotonin$_{1A}$ receptor in a pure POPC membrane (right). For each system, 100 snapshots of the behavior of ECL1 (colored cyan) are shown. The Cα of the K101 residue in the wild-type serotonin$_{1A}$ receptor is depicted in van der Waals representation (dark blue). (**B**) K101A mutation alters ECL1 conformational dynamics. Frequencies of helical states for individual residues in the ECL1 for the wild-type and K101A mutant serotonin$_{1A}$ receptor in cholesterol-containing membranes (POPC/chol) or membranes without cholesterol (POPC) (left). Helical states of the ECL1 in the K101A mutant are shown in the right. The Cα of A101 (K101A) residue is depicted in van der Waals representation (dark blue). Note that the helicity of the wild-type receptor is negligible and not visible in the plot. (**C**) Altered behavior of ECL1 correlates with changes in ECL2 and ECL3 dynamics. Locations of ECL1 (cyan), ECL2 (red), and ECL3 (orange) in the serotonin$_{1A}$ receptor are shown in the left. Plots of RMSF as a measure of the dynamics of ECL1, ECL2, and ECL3 for the wild-type and K101A mutant serotonin$_{1A}$ receptor in cholesterol-containing membranes (POPC/chol) or membranes without cholesterol (POPC) are shown in the right. See Materials and Methods for further details.

Downloaded from http://advances.sciencemag.org/ on July 23, 2021

To address the molecular mechanism of cholesterol sensitivity of the serotonin$_{1A}$ receptor and the role of the K101 residue in mediating this sensitivity, we carried out all-atom MD simulations. Our analysis showed that cholesterol tightly binds between TM1 and TM2 by establishing polar contacts with K101 that leads to stabilization of ECL1. While this manuscript was being revised, an active-state structure of the serotonin$_{1A}$ receptor coupled to G$_i$ was published (*47*). This structure revealed a cocrystallized cholesterol molecule in a position almost identical to the one observed in our MD simulations (see fig. S7). This strongly validates our observations and reinforces the molecular mechanism for cholesterol sensitivity of the serotonin$_{1A}$ receptor that we proposed. The link between ECL1 stability and cholesterol sensitivity was further supported by simulations of the K101A mutant, which exhibited cholesterol-insensitive signaling (Fig. 4 and fig. S4). This prompted us to speculate that ECL1 dynamics and receptor signaling could be structurally associated. Our simulations revealed that ECL1 dynamics (fluctuations) could propagate to other ECL regions, which is indicated by similar higher values of RMSF for ECL2 and ECL3. These results highlight that changes within ECL1 could lead to global structural changes in the receptor that are responsible for the observed cholesterol sensitivity. Our results assume significance in the backdrop of growing evidence on the role of ECL dynamics in regulating the function of several GPCRs (*48*–*51*) that include the closely related serotonin$_{2B}$ (*52*) and serotonin$_{2A}$ (*53*) receptors. These results point toward the role of membrane cholesterol in inducing global structural changes that could propagate via ECLs and facilitate signaling conformations of GPCRs. In addition to the CRAC motifs, the presence of other cholesterol-binding sites (e.g., cholesterol consensus motif) has previously been reported for the serotonin$_{1A}$ receptor (*28*). It is important to note that our findings do not rule out a functional interplay between different cholesterol-binding sites. Future work could provide more insight into this additional level of complexity.

Together, our results show that the cholesterol sensitivity exhibited by the serotonin$_{1A}$ receptor is mediated by the K101 residue in the evolutionarily conserved CRAC motif I. The specific interaction of cholesterol with membrane proteins has been implicated in modulating the function of several important GPCRs. Identification of cholesterol recognition motifs such as CRAC in GPCRs has enabled us to explore the mechanistic basis of GPCR-cholesterol interaction.

In general, the presence of CRAC motifs in a transmembrane region suggests the "possibility" of cholesterol interaction with the receptor. However, it is advisable to exercise caution before attributing cholesterol dependence in receptor function to the mere presence of these motifs. For example, an earlier study of bacterial genomes (*Streptococcus agalactiae*, *Staphylococcus aureus*, and *Escherichia coli*) reported an average occurrence rate of two to three CRAC motifs in diverse proteins that do not interact with cholesterol (*54*). In addition, the neurotensin type 1 receptor has CRAC motifs in its TM1 and TM6. However, this receptor does not display any change in downstream signaling upon cholesterol depletion (*55*). Conversely, in a recent crystal structure of the oxytocin receptor, which exhibits cholesterol-sensitive function, a single cholesterol molecule was observed at a site that did not harbor a CRAC motif (*56*). Experimental evidences such as the ones reported in our present work are therefore crucial in establishing the molecular basis underlying the role of CRAC motifs in conferring cholesterol sensitivity to GPCRs.

MATERIALS AND METHODS

Materials

Bovine serum albumin, custom DNA oligos, EDTA, doxycycline hyclate, forskolin, hygromycin B solution, 3-isobutyl-1-methylxanthine (IBMX), MβCD, phenylmethylsulfonyl fluoride (PMSF), penicillin, streptomycin, gentamycin sulfate, serotonin, and tris were obtained from Sigma Chemical Co. (St. Louis, MO). DMEM/F-12 [Dulbecco's modified Eagle's medium:nutrient mixture F-12 (Ham) (1:1)] and fetal calf serum (FCS) were obtained from Invitrogen/Life Technologies (Grand Island, NY). Bicinchoninic acid (BCA) assay reagent was from Pierce (Rockford, IL). Anti-myc antibody Alexa Fluor 488 conjugate was purchased from Millipore (Bedford, MA). Amplex Red cholesterol assay kit was purchased from Molecular Probes/Invitrogen (Eugene, OR). HTRF cAMP-G$_i$ assay kit was purchased from CisBio Bioassays (Codolet, France). QuikChange Lightning Multi Site-Directed Mutagenesis Kit was purchased from Agilent Technologies (Santa Clara, CA). Flp-In 293 T-REx cell lines and Lipofectamine 2000 were purchased from Invitrogen (Eugene, OR). All other chemicals used were of the highest available purity. Water was purified through a Millipore (Bedford, MA) Milli-Q system and used throughout.

Generation of CRAC motif mutants

Four single mutants [(i) Y96S (the tyrosine residue in the CRAC motif I replaced by a serine), (ii) K101A (the lysine residue in the CRAC motif I replaced by an alanine), (iii) Y215S (the tyrosine residue in the CRAC motif II replaced by a serine), and (iv) R220A (the arginine residue in the CRAC motif II replaced by an alanine)] and two double mutants [(v) Y96S + Y215S and (vi) K101A + R220A] were generated. The point mutations were carried out using the QuikChange Lightning Multi Site-Directed Mutagenesis Kit as per the manufacturer's protocol and verified by DNA sequencing. The primers used for the generation of the point mutations are as follows: Y96S_sense, 5′-CCC ATG GCC GCG CTG AGT CAG GTG CTC AAC AA-3′; K101A_sense, 5′-GTA TCA GGT GCT CAA CGC GTG GAC ACT GGG CCA G-3′; Y215S_sense, 5′-TGC TCA TGC TGG TTC TCA GTG GGC GCA TAT TCC GAG-3′; R220A_sense, 5′-TCT CTA TGG GCG CAT ATT CGC AGC TGC GCG CTT C-3′.

Generation of stable cell lines

Stable HEK-293 cell lines with tetracycline-inducible expression of N-terminal 6xHis and Myc-tagged serotonin$_{1A}$ receptor and N-terminal 6xHis and Myc-tagged serotonin$_{1A}$ receptor with mutations in CRAC motifs I and/or II were generated using the Flp-In T-REx System (*57*). The Flp-In T-REx System consists of Flp-In T-REx 293 cells containing a Flp recombination target (FRT) site and expressing the tetracycline repressor (tet repressor), inducible expression vector pcDNA5/FRT/TO, and pOG44 Flp recombinase expression vector. The complementary DNA sequences encoding the N-terminal 6xHis and Myc-tagged serotonin$_{1A}$ receptor and those with the CRAC motif mutations were subcloned into pcDNA5/FRT/TO vector between Kpn I and Bam HI restriction sites after polymerase chain reaction amplification using the primers KPNIHISF (5′-CCG CTA GGT ACC ATG CAT CAT CAC-3′) and HTR1ABAMHIR (5′-TCA TCA GGA TCC TCA CTG GCG GCA GAA CTT-3′). The resulting constructs, after sequence verification, were transfected into Flp-In T-REx 293 cells along with pOG44 Flp recombinase expression vector by lipofectamine-mediated transfection, and the stable colonies were selected using hygromycin B.

Downloaded from http://advances.sciencemag.org/ on July 23, 2021

Cell culture

HEK-293 cells stably expressing N-terminal myc-tagged serotonin$_{1A}$ receptor and its mutants were maintained in DMEM/F-12 medium with 10% (v/v) FCS containing penicillin (60 μg/ml), streptomycin (50 μg/ml), gentamicin sulfate (50 μg/ml), and hygromycin B (250 μg/ml) (complete medium) in a humidified atmosphere with 5% CO_2 at 37°C. The culture medium was supplemented with doxycycline (1 μg/ml) for 24 hours to induce receptor expression before experiments.

Confocal microscopic imaging

Cells were plated on glass coverslips and grown in complete medium in a humidified atmosphere with 5% CO_2 at 37°C. To obtain representative confocal microscopic images for plasma membrane localization of the receptor, cells were washed with phosphate-buffered saline (PBS) and fixed with 4% (w/v) formaldehyde. Cells were then labeled with anti-myc antibody Alexa Fluor 488 conjugate (1:100 dilution) in PBS containing 2% (v/v) FCS for 60 min, washed, and mounted. Images were acquired on a Zeiss LSM 880 confocal microscope (Jena, Germany). N-terminal myc-tagged serotonin$_{1A}$ receptors were imaged by exciting anti-myc antibody Alexa Fluor 488 conjugate at 488 nm and collecting emission from 495 to 560 nm. Images were acquired with a 63×/1.4 NA oil immersion objective under 1 airy condition.

Flow cytometric analysis of receptor expression level

HEK-293 cell lines expressing the wild-type and CRAC motif mutant serotonin$_{1A}$ receptor were collected in PBS on ice. Cells were fixed with 4% (w/v) formaldehyde in PBS for 30 min and labeled with anti-myc antibody Alexa Fluor 488 conjugate (1:100 dilution) in PBS containing 2% (v/v) FCS for 60 min on ice. Cells were washed and suspended in PBS. A MoFlo XDP flow cytometer (Brea, CA) was used to acquire data from 10,000 cells. Alexa Fluor 488 was excited at 488 nm, and emission was collected using a 529/28-nm bandpass filter. The plasma membrane–associated receptor population was measured in terms of mode count values using the Summit analysis software version 5.4.0.

Membrane cholesterol depletion and estimation

Membrane cholesterol from cells was depleted as described previously (*13*). Briefly, cells were grown in complete medium for 48 hours followed by incubation in serum-free DMEM/F-12 (1:1) medium for 3 hours in a humidified atmosphere with 5% CO_2 at 37°C. Membrane cholesterol was depleted using 10 mM MβCD in serum-free medium at 37°C for 30 min. Cells were subsequently washed with PBS, and membranes were prepared. Cholesterol content of cell membranes was estimated using the Amplex Red cholesterol assay kit (*58*). Cholesterol levels were normalized to the total protein content of cell membranes.

Cell membrane preparation

Cell membranes were isolated from control and MβCD-treated cells as described previously (*59*). Briefly, cells were collected in ice-cold hypotonic buffer containing 10 mM tris, 5 mM EDTA, and 0.1 mM PMSF (pH 7.4). Cells were then homogenized for 10 s at 4°C with a Polytron homogenizer at maximum speed. The cell lysate was centrifuged at 500*g* for 10 min at 4°C, and the resulting postnuclear supernatant was centrifuged at 40,000*g* for 30 min at 4°C. The final pellet was resuspended in 50 mM tris buffer (pH 7.4), homogenized using a handheld Dounce homogenizer, and used for membrane cholesterol estimation. The total protein concentration in isolated membranes was measured using BCA assay (*60*).

Cellular signaling assay

HEK-293 cells stably expressing wild-type or CRAC motif mutant serotonin$_{1A}$ receptors were plated at a density of ~5×10^4 cells in six-well plates and grown in complete medium for 48 hours followed by incubation in serum-free DMEM/F-12 (1:1) medium for 3 hours. After treatment with 10 mM MβCD in serum-free medium at 37°C for 30 min, cells were rinsed with PBS and incubated with 50 μM IBMX (basal), 50 μM IBMX/10 μM forskolin (forskolin-stimulated), or 50 μM IBMX/10 μM forskolin/10 μM serotonin (agonist treatment) for 30 min at 37°C. The phosphodiesterase inhibitor IBMX was present during all treatments to prevent breakdown of cAMP. After discarding media, cells were washed once with PBS. Cells were subsequently detached using a cell scraper, counted, and added at 6000 cells per well to a low-volume HTRF 96-well plate (CisBio Bioassays, Codolet, France). The ability of wild-type and mutant serotonin$_{1A}$ receptors to inhibit the forskolin-stimulated increase in cAMP levels in cells was assessed using the FRET-based HTRF cAMP-G_i assay kit (CisBio Bioassays, Codolet, France) as specified by the manufacturer (*36*). Fluorescence was measured at 620 nm (cAMP-cryptate donor emission) and 655 nm (anti–cAMP-d2 acceptor emission) upon excitation of the donor at 320 nm using an EnSpire multimode plate reader (PerkinElmer, Waltham, MA). cAMP levels were calculated as a ratio of the acceptor and donor emission. Values for serotonin-induced cAMP reduction were normalized and expressed as a percentage of the cAMP content in cells stimulated with forskolin.

Statistical analysis

Statistical significance of data was analyzed using Student's two-tailed unpaired *t* test using GraphPad Prism software version 4.0 (San Diego, CA). SigmaPlot version 11.0 (Systat Software Inc., San Jose, CA) was used to generate plots.

System generation for MD simulations

For studying the serotonin$_{1A}$ receptor in complex with an agonist, we simulated an active conformation of the receptor. A model of the serotonin$_{1A}$ receptor in this conformation was retrieved from GPCRdb (ClassA_5ht1a_human_Active_6G79_2019-09-03_GPCRdb) (*61*). This structural model was based on the closely related serotonin$_{1B}$ receptor in complex with the heterotrimeric G_o protein [Protein Data Bank (PDB) ID: 6G79]. The ligand (serotonin) was placed within the model using docking and available mutational data. Protonation states were calculated at pH 7.4 using PROPKA (*62*). The conserved D2.50 residue was kept protonated, due to the receptor being in an active state. The receptor-ligand complexes thus obtained were embedded within a POPC or POPC containing 33 mole percent cholesterol (POPC/chol) membrane and solvated using TIP3P waters in CHARMM-GUI (*63*). Ionic strength of the systems was kept at 0.15 M using NaCl ions. Protein and lipid parameters were obtained from Charmm36m (*64*) and Charmm36 (*65*), respectively.

Simulation protocol and analysis

Generated systems were simulated using the ACEMD package (*66*). The simulation protocol included an equilibration step of 50 ns under a condition of constant pressure (1.01325 bar, NPT) to ensure proper

Downloaded from http://advances.sciencemag.org/ on July 23, 2021

lipid packing. During this step, the backbone of the receptor was constrained, and the time step was set at 2 fs. The pressure was kept constant using the Berendsen barostat (*67*). This was followed by four production runs of 2 μs for each system with a time step of 4 fs under conditions of constant volume (NVT). During both NPT and NVT runs, temperature was maintained constant using the Langevin thermostat (*68*). Van der Waals and short-range electrostatic interactions were implemented with a cutoff of 9 Å and a switching potential applied at 7.5 Å, and long-range electrostatic interactions were approximated using the particle mesh Ewald method (*69*). Analysis of systems was carried out using VMD (*70*). All volumetric occupancy maps were plotted at isovalue of 0.2. Helicity of ECL2 was assessed using the VMD Timeline plugin. Parameters for the ligand were assigned from the CGenFF force field automatically by the ParamChem tool implemented in CHARMM-GUI (*71*, *72*).

SUPPLEMENTARY MATERIALS

Supplementary material for this article is available at http://advances.sciencemag.org/cgi/content/full/7/30/eabh2922/DC1

View/request a protocol for this paper from *Bio-protocol*.

REFERENCES AND NOTES

1. W. I. Weis, B. K. Kobilka, The molecular basis of G protein-coupled receptor activation. *Annu. Rev. Biochem.* **87**, 897–919 (2018).
2. H. C. S. Chan, Y. Li, T. Dahoun, H. Vogel, S. Yuan, New binding sites, new opportunities for GPCR drug discovery. *Trends Biochem. Sci.* **44**, 312–330 (2019).
3. F. R. Maxfield, G. van Meer, Cholesterol, the central lipid of mammalian cells. *Curr. Opin. Cell Biol.* **22**, 422–429 (2010).
4. J. Fantini, F. J. Barrantes, How cholesterol interacts with membrane proteins: An exploration of cholesterol-binding sites including CRAC, CARC, and tilted domains. *Front. Physiol.* **4**, 31 (2013).
5. C. Wang, A. Ralko, Z. Ren, A. Rosenhouse-Dantsker, X. Yang, Modes of cholesterol binding in membrane proteins: A joint analysis of 73 crystal structures. *Adv. Exp. Med. Biol.* **1135**, 67–86 (2019).
6. T. J. Pucadyil, A. Chattopadhyay, Role of cholesterol in the function and organization of G-protein coupled receptors. *Prog. Lipid Res.* **45**, 295–333 (2006).
7. Y. D. Paila, A. Chattopadhyay, Membrane cholesterol in the function and organization of G-protein coupled receptors. *Subcell. Biochem.* **51**, 439–466 (2010).
8. J. Oates, A. Watts, Uncovering the intimate relationship between lipids, cholesterol and GPCR activation. *Curr. Opin. Struct. Biol.* **21**, 802–807 (2011).
9. G. Gimpl, Interaction of G protein coupled receptors and cholesterol. *Chem. Phys. Lipids* **199**, 61–73 (2016).
10. M. Jafurulla, G. A. Kumar, B. D. Rao, A. Chattopadhyay, A critical analysis of molecular mechanisms underlying membrane cholesterol sensitivity of GPCRs. *Adv. Exp. Med. Biol.* **1115**, 21–52 (2019).
11. T. J. Pucadyil, S. Kalipatnapu, A. Chattopadhyay, The serotonin$_{1A}$ receptor: A representative member of the serotonin receptor family. *Cell. Mol. Neurobiol.* **25**, 553–580 (2005).
12. C. P. Müller, R. J. Carey, J. P. Huston, M. A. De Souza Silva, Serotonin and psychostimulant addiction: Focus on 5-HT$_{1A}$-receptors. *Prog. Neurobiol.* **81**, 133–178 (2007).
13. T. J. Pucadyil, A. Chattopadhyay, Cholesterol modulates ligand binding and G-protein coupling to serotonin$_{1A}$ receptors from bovine hippocampus. *Biochim. Biophys. Acta* **1663**, 188–200 (2004).
14. T. J. Pucadyil, A. Chattopadhyay, Cholesterol depletion induces dynamic confinement of the G-protein coupled serotonin$_{1A}$ receptor in the plasma membrane of living cells. *Biochim. Biophys. Acta* **1768**, 655–668 (2007).
15. Y. D. Paila, M. R. V. S. Murty, M. Vairamani, A. Chattopadhyay, Signaling by the human serotonin$_{1A}$ receptor is impaired in cellular model of Smith-Lemli-Opitz syndrome. *Biochim. Biophys. Acta* **1778**, 1508–1516 (2008).
16. S. Shrivastava, T. J. Pucadyil, Y. D. Paila, S. Ganguly, A. Chattopadhyay, Chronic cholesterol depletion using statin impairs the function and dynamics of human serotonin$_{1A}$ receptors. *Biochemistry* **49**, 5426–5435 (2010).
17. S. Ganguly, A. H. A. Clayton, A. Chattopadhyay, Organization of higher-order oligomers of the serotonin$_{1A}$ receptor explored utilizing homo-FRET in live cells. *Biophys. J.* **100**, 361–368 (2011).
18. M. Jafurulla, B. D. Rao, S. Sreedevi, J.-M. Ruysschaert, D. F. Covey, A. Chattopadhyay, Stereospecific requirement of cholesterol in the function of the serotonin$_{1A}$ receptor. *Biochim. Biophys. Acta* **1838**, 158–163 (2014).
19. X. Prasanna, D. Sengupta, A. Chattopadhyay, Cholesterol-dependent conformational plasticity in GPCR dimers. *Sci. Rep.* **6**, 31858 (2016).
20. H. Chakraborty, M. Jafurulla, A. H. A. Clayton, A. Chattopadhyay, Exploring oligomeric state of the serotonin$_{1A}$ receptor utilizing photobleaching image correlation spectroscopy: Implications for receptor function. *Faraday Discuss.* **207**, 409–421 (2018).
21. G. A. Kumar, A. Chattopadhyay, Statin-induced chronic cholesterol depletion switches GPCR endocytosis and trafficking: Insights from the serotonin$_{1A}$ receptor. *ACS Chem. Nerosci.* **11**, 453–465 (2020).
22. P. Sarkar, M. Jafurulla, S. Bhowmick, A. Chattopadhyay, Structural stringency and optimal nature of cholesterol requirement in the function of the serotonin$_{1A}$ receptor. *J. Membr. Biol.* **253**, 445–457 (2020).
23. V. Cherezov, D. M. Rosenbaum, M. A. Hanson, S. G. F. Rasmussen, F. S. Thian, T. S. Kobilka, H. J. Choi, P. Kuhn, W. I. Weis, B. K. Kobilka, R. C. Stevens, High-resolution crystal structure of an engineered human β_2-adrenergic G protein-coupled receptor. *Science* **318**, 1258–1265 (2007).
24. M. A. Hanson, V. Cherezov, M. T. Griffith, M. T. Roth, V.-P. Jaakola, E. Y. T. Chien, J. Velasquez, P. Kuhn, R. C. Stevens, A specific cholesterol binding site is established by the 2.8 Å structure of the human β_2-adrenergic receptor. *Structure* **16**, 897–905 (2008).
25. Y. Wang, Z. Yu, W. Xiao, S. Lu, J. Zhang, Allosteric binding sites at the receptor-lipid bilayer interface: Novel targets for GPCR drug discovery. *Drug Discov. Today* **26**, 690–703 (2021).
26. R. M. Epand, Cholesterol and the interaction of proteins with membrane domains. *Prog. Lipid Res.* **45**, 279–294 (2006).
27. J. Fantini, R. M. Epand, F. J. Barrantes, Cholesterol-recognition motifs in membrane proteins. *Adv. Exp. Med. Biol.* **1135**, 3–25 (2019).
28. P. Sarkar, A. Chattopadhyay, Cholesterol interaction motifs in G protein-coupled receptors: Slippery hot spots? *Wiley Interdiscip. Rev. Syst. Biol. Med.* **12**, e1481 (2020).
29. H. Li, V. Papadopoulos, Peripheral-type benzodiazepine receptor function in cholesterol transport. Identification of a putative cholesterol recognition/interaction amino acid sequence and consensus pattern. *Endocrinology* **139**, 4991–4997 (1998).
30. M. Jafurulla, S. Tiwari, A. Chattopadhyay, Identification of cholesterol recognition amino acid consensus (CRAC) motif in G-protein coupled receptors. *Biochem. Biophys. Res. Commun.* **404**, 569–573 (2011).
31. J. Fantini, C. Di Scala, C. J. Baier, F. J. Barrantes, Molecular mechanisms of protein-cholesterol interactions in plasma membranes: Functional distinction between topological (tilted) and consensus (CARC/CRAC) domains. *Chem. Phys. Lipids* **199**, 52–60 (2016).
32. G. A. Kumar, P. Sarkar, M. Jafurulla, S. P. Singh, G. Srinivas, G. Pande, A. Chattopadhyay, Exploring endocytosis and intracellular trafficking of the human serotonin$_{1A}$ receptor. *Biochemistry* **58**, 2628–2641 (2019).
33. S. Shrivastava, P. Sarkar, P. Preira, L. Salomé, A. Chattopadhyay, Role of actin cytoskeleton in dynamics and function of the serotonin$_{1A}$ receptor. *Biophys. J.* **118**, 944–956 (2020).
34. A. Malmberg, P. G. Strange, Site-directed mutations in the third intracellular loop of the serotonin 5-HT$_{1A}$ receptor alter G protein coupling from G_i to G_s in a ligand-dependent manner. *J. Neurochem.* **75**, 1283–1293 (2000).
35. J. R. Raymond, C. L. Olsen, T. W. Gettys, Cell-specific physical and functional coupling of human 5-HT$_{1A}$ receptors to inhibitory G protein .alpha.-subunits and lack of coupling to $G_{\alpha s}$. *Biochemistry* **32**, 11064–11073 (1993).
36. J.-L. Tardieu, Selecting a cyclic AMP kit for assaying GPCR target activation. *Nat. Methods* **5**, iii–iv (2008).
37. R. J. Ward, J. D. Pediani, K. G. Harikumar, L. J. Miller, G. Milligan, Spatial intensity distribution analysis quantifies the extent and regulation of homodimerization of the secretin receptor. *Biochem. J.* **474**, 1879–1895 (2017).
38. G. Gimpl, K. Burger, F. Fahrenholz, Cholesterol as modulator of receptor function. *Biochemistry* **36**, 10959–10974 (1997).
39. R. Zidovetzki, I. Levitan, Use of cyclodextrins to manipulate plasma membrane cholesterol content: Evidence, misconceptions and control strategies. *Biochim. Biophys. Acta* **1768**, 1311–1324 (2007).
40. S. Mahammad, I. Parmryd, Cholesterol depletion using methyl-β-cyclodextrin. *Methods Mol. Biol.* **1232**, 91–102 (2015).
41. N. Jamin, J.-M. Neumann, M. A. Ostuni, T. K. N. Vu, Z.-X. Yao, S. Murail, J.-C. Robert, C. Giatzakis, V. Papadopoulos, J.-J. Lacapère, Characterization of the cholesterol recognition amino acid consensus sequence of the peripheral-type benzodiazepine receptor. *Mol. Endocrinol.* **19**, 588–594 (2005).
42. R. M. Epand, B. G. Sayer, R. F. Epand, Caveolin scaffolding region and cholesterol-rich domains in membranes. *J. Mol. Biol.* **345**, 339–350 (2005).
43. R. Nygaard, Y. Zou, R. O. Dror, T. J. Mildorf, D. H. Arlow, A. Manglik, A. C. Pan, C. W. Liu, J. J. Fung, M. P. Bokoch, F. S. Thian, T. S. Kobilka, D. E. Shaw, L. Mueller, R. S. Prosser, B. K. Kobilka, The dynamic process of β_2-adrenergic receptor activation. *Cell* **152**, 532–542 (2013).
44. P. Sarkar, S. Mozumder, A. Bej, S. Mukherjee, J. Sengupta, A. Chattopadhyay, Structure, dynamics and lipid interactions of serotonin receptors: Excitements and challenges. *Biophys. Rev.* **13**, 101–122 (2021).

Downloaded from http://advances.sciencemag.org/ on July 23, 2021

45. D. A. Kelkar, A. Chattopadhyay, Membrane interfacial localization of aromatic amino acids and membrane protein function. *J. Biosci.* **31**, 297–302 (2006).
46. M. B. Ulmschneider, M. S. P. Sansom, Amino acid distributions in integral membrane protein structures. *Biochim. Biophys. Acta* **1512**, 1–14 (2001).
47. P. Xu, S. Huang, H. Zhang, C. Mao, X. E. Zhou, X. Cheng, I. A. Simon, D. D. Shen, H. Y. Yen, C. V. Robinson, K. Harpsøe, B. Svensson, J. Guo, H. Jiang, D. E. Gloriam, K. Melcher, Y. Jiang, Y. Zhang, H. E. Xu, Structural insights into the lipid and ligand regulation of serotonin receptors. *Nature* **592**, 469–473 (2021).
48. M. C. Peeters, G. J. van Westen, Q. Li, A. P. IJzerman, Importance of the extracellular loops in G protein-coupled receptors for ligand recognition and receptor activation. *Trends Pharmacol. Sci.* **32**, 35–42 (2011).
49. M. Wheatley, D. Wootten, M. T. Conner, J. Simms, R. Kendrick, R. T. Logan, D. R. Poyner, J. Barwell, Lifting the lid on GPCRs: The role of extracellular loops. *Br. J. Pharmacol.* **165**, 1688–1703 (2012).
50. N. R. Latorraca, A. J. Venkatakrishnan, R. O. Dror, GPCR dynamics: Structures in motion. *Chem. Rev.* **117**, 139–155 (2017).
51. S. Pal, A. Chattopadhyay, Extramembranous regions in G protein-coupled receptors: Cinderella in receptor biology? *J. Membr. Biol.* **252**, 483–497 (2019).
52. D. Wacker, S. Wang, J. D. McCorvy, R. M. Betz, A. J. Venkatakrishnan, A. Levit, K. Lansu, Z. L. Schools, T. Che, D. E. Nichols, B. K. Shoichet, R. O. Dror, B. L. Roth, Crystal structure of an LSD-bound human serotonin receptor. *Cell* **168**, 377–389.e12 (2017).
53. A. Iglesias, M. Cimadevila, R. A. la Fuente, M. Martí-Solano, M. I. Cadavid, M. Castro, J. Selent, M. I. Loza, J. Brea, Serotonin 2_A receptor disulfide bridge integrity is crucial for ligand binding to different signalling states but not for its homodimerization. *Eur. J. Pharmacol.* **815**, 138–146 (2017).
54. M. Palmer, Cholesterol and the activity of bacterial toxins. *FEMS Microbiol. Lett.* **238**, 281–289 (2004).
55. J. Oates, B. Faust, H. Attrill, P. Harding, M. Orwick, A. Watts, The role of cholesterol on the activity and stability of neurotensin receptor 1. *Biochim. Biophys. Acta* **1818**, 2228–2233 (2012).
56. Y. Waltenspühl, J. Schöppe, J. Ehrenmann, L. Kummer, A. Plückthun, Crystal structure of the human oxytocin receptor. *Sci. Adv.* **6**, eabb5419 (2020).
57. R. J. Ward, E. Alvarez-Curto, G. Milligan, Using the Flp-In™ T-Rex™ system to regulate GPCR expression. *Methods Mol. Biol.* **746**, 21–31 (2011).
58. D. M. Amundson, M. Zhou, Fluorometric method for the enzymatic determination of cholesterol. *J. Biochem. Biophys. Methods* **38**, 43–52 (1999).
59. S. Kalipatnapu, T. J. Pucadyil, K. G. Harikumar, A. Chattopadhyay, Ligand binding characteristics of the human serotonin$_{1A}$ receptor heterologously expressed in CHO cells. *Biosci. Rep.* **24**, 101–115 (2004).
60. P. K. Smith, R. I. Krohn, G. T. Hermanson, A. K. Mallia, F. H. Gartner, M. D. Provenzano, E. K. Fujimoto, N. M. Goeke, B. J. Olson, D. C. Klenk, Measurement of protein using bicinchoninic acid. *Anal. Biochem.* **150**, 76–85 (1985).
61. G. Pándy-Szekeres, C. Munk, T. M. Tsonkov, S. Mordalski, K. Harpsøe, A. S. Hauser, A. J. Bojarski, D. E. Gloriam, GPCRdb in 2018: Adding GPCR structure models and ligands. *Nucleic Acids Res.* **46**, D440–D446 (2018).
62. H. Li, A. D. Robertson, J. H. Jensen, Very fast empirical prediction and rationalization of protein pKa values. *Proteins* **61**, 704–721 (2005).
63. S. Jo, T. Kim, V. G. Iyer, W. Im, CHARMM-GUI: A web-based graphical user interface for CHARMM. *J. Comput. Chem.* **29**, 1859–1865 (2008).
64. J. Huang, S. Rauscher, G. Nawrocki, T. Ran, M. Feig, B. L. de Groot, H. Grubmüller, A. D. MacKerell Jr., CHARMM36m: An improved force field for folded and intrinsically disordered proteins. *Nat. Methods* **14**, 71–73 (2017).
65. J. B. Klauda, R. M. Venable, J. A. Freites, J. W. O'Connor, D. J. Tobias, C. Mondragon-Ramirez, I. Vorobyov, A. D. MacKerell Jr., R. W. Pastor, Update of the CHARMM all-atom additive force field for lipids: Validation on six lipid types. *J. Phys. Chem. B* **114**, 7830–7843 (2010).
66. M. J. Harvey, G. Giupponi, G. De Fabritiis, ACEMD: Accelerating biomolecular dynamics in the microsecond time scale. *J. Chem. Theory Comput.* **5**, 1632–1639 (2009).
67. H. J. C. Berendsen, J. P. M. Postma, W. F. Van Gunsteren, A. Dinola, J. R. Haak, Molecular dynamics with coupling to an external bath. *J. Chem. Phys.* **81**, 3684–3690 (1984).
68. G. S. Grest, K. Kremer, Molecular dynamics simulation for polymers in the presence of a heat bath. *Phys. Rev. A* **33**, 3628–3631 (1986).
69. T. Darden, D. York, L. Pedersen, Particle mesh Ewald: An *N*·log(*N*) method for Ewald sums in large systems. *J. Chem. Phys.* **98**, 10089–10092 (1993).
70. W. Humphrey, A. Dalke, K. Schulten, VMD: Visual molecular dynamics. *J. Mol. Graph.* **14**, 33–38 (1996).
71. K. Vanommeslaeghe, E. Hatcher, C. Acharya, S. Kundu, S. Zhong, J. Shim, E. Darian, O. Guvench, P. Lopes, I. Vorobyov, A. D. Mackerell Jr., CHARMM general force field: A force field for drug-like molecules compatible with the CHARMM all-atom additive biological force fields. *J. Comput. Chem.* **31**, 671–690 (2010).
72. W. Yu, X. He, K. Vanommeslaeghe, A. D. MacKerell Jr., Extension of the CHARMM general force field to sulfonyl-containing compounds and its utility in biomolecular simulations. *J. Comput. Chem.* **33**, 2451–2468 (2012).

Acknowledgments: We thank M. M. Panicker for helpful discussion, G. Srinivas for help with acquiring flow cytometric data, and members of the Chattopadhyay laboratory for critically reading the manuscript and for comments. **Funding:** This work was supported by a SERB Distinguished Fellowship grant (Department of Science and Technology, Government of India) to A.C. and core support from the CSIR-Centre for Cellular and Molecular Biology. J.S. acknowledges financial support from the Instituto de Salud Carlos III FEDER (PI15/00460 and PI18/00094) and the ERA-NET NEURON and Ministry of Economy, Industry, and Competitiveness (AC18/00030). G.A.K. was supported by the award of a Senior Research Fellowship from the Council of Scientific and Industrial Research (CSIR) and as a senior project associate by a CSIR FBR grant to A.C. (MLP 0146). P.S. thanks the CSIR for the award of a Shyama Prasad Mukherjee Fellowship. T.M.S. acknowledges support from the National Center of Science, Poland, grant 2017/27/N/NZ2/02571 and is currently employed in InterAx Biotech AG, 5234 Villigen, Switzerland. S.P.S. thanks the National Centre for Biological Sciences for the award of a Senior Research Fellowship. **Author contributions:** G.A.K. and P.S. performed experiments. T.M.S. carried out MD simulations under the supervision of J.S. G.A.K., P.S., T.M.S., J.S., and A.C. analyzed data. S.P.S. generated CRAC motif mutants. G.A.K., P.S., T.M.S., M.J., J.S., and A.C. designed experiments. G.A.K., P.S., T.M.S., J.S., and A.C. wrote the manuscript. A.C. edited the manuscript, organized access to research facilities and funding, and provided overall supervision and mentoring. **Competing interests:** The authors declare that they have no competing interests. **Data and materials availability:** All data needed to evaluate the conclusions in the paper are present in the paper and/or the Supplementary Materials. Additional data related to this paper may be requested from the authors.

Submitted 27 February 2021
Accepted 9 June 2021
Published 23 July 2021
10.1126/sciadv.abh2922

Citation: G. A. Kumar, P. Sarkar, T. M. Stepniewski, M. Jafurulla, S. P. Singh, J. Selent, A. Chattopadhyay, A molecular sensor for cholesterol in the human serotonin$_{1A}$ receptor. *Sci. Adv.* **7**, eabh2922 (2021).

Downloaded from http://advances.sciencemag.org/ on July 23, 2021

Science Advances

A molecular sensor for cholesterol in the human serotonin$_{1A}$ receptor

G. Aditya Kumar, Parijat Sarkar, Tomasz Maciej Stepniewski, Md. Jafurulla, Shishu Pal Singh, Jana Selent and Amitabha Chattopadhyay

Sci Adv **7** (30), eabh2922.
DOI: 10.1126/sciadv.abh2922

ARTICLE TOOLS http://advances.sciencemag.org/content/7/30/eabh2922

SUPPLEMENTARY MATERIALS http://advances.sciencemag.org/content/suppl/2021/07/19/7.30.eabh2922.DC1

REFERENCES This article cites 72 articles, 4 of which you can access for free
http://advances.sciencemag.org/content/7/30/eabh2922#BIBL

PERMISSIONS http://www.sciencemag.org/help/reprints-and-permissions

Use of this article is subject to the Terms of Service

Science Advances (ISSN 2375-2548) is published by the American Association for the Advancement of Science, 1200 New York Avenue NW, Washington, DC 20005. The title *Science Advances* is a registered trademark of AAAS.

Copyright © 2021 The Authors, some rights reserved; exclusive licensee American Association for the Advancement of Science. No claim to original U.S. Government Works. Distributed under a Creative Commons Attribution NonCommercial License 4.0 (CC BY-NC).

Downloaded from http://advances.sciencemag.org/ on July 23, 2021